

Per Sub-band Tone Reservation Scheme for Universal Filtered Multi-Carrier Signal

Laabidi Mounira, and Bouallegue Ridha

Abstract—Fifth generation (5G) applications like Internet of Things (IoT), Enhanced Mobile Broadband (eMBB), Cognitive Radios (CR), Vehicle to Vehicle (V2V) and Machine to Machine (M2M) communication put new demands on the network in terms of low latency, ultra-reliable communication and efficiency when transmitting very small bursts. One new contender that makes its appearance recently is the Universal Filtered Multi-Carrier (UFMC). UFMC is a potential candidate to meet the requirements of 5G upcoming applications. This related waveform encounters the peak-to-average power ratio (PAPR) issue arising from the usage of multi-carrier transmission. In this investigation, two PAPR reduction techniques, called Per Sub-band Tone Reservation (PSTR) scheme to alleviate PAPR in UFMC systems are suggested. The first one is a pre-filtering PSTR scheme that uses the least squares approximation (LSA) algorithm to calculate the optimization factor (μ) and the second one is a post-filtering method. The concept of this proposal lies on the use of peaks reductions Tone to carry the correctional signal that reduces the high peaks of each sub-band individually. To shed light on UFMC as a potential waveform for 5G upcoming application, a comparison with OFDM modulation is done.

Keywords—UFMC, PAPR, PSTR, Fifth generation (5G)

I. INTRODUCTION

Fifth generation (5G) will support various use cases like Enhanced Mobile Broadband (eMBB), high-reliability services and wide area Internet of Thing (IoT) (1) (2)(3)-(4). Higher throughput and higher spectral efficiency are required for eMBB. Regarding IoT, short data bursts and long device battery life are expected. Lower latency and lower packet loss rate to ensure higher-reliability services are also some 5G requirements (5) (6) (7).

The Orthogonal Frequency Division Multiplexing (OFDM) (8) (9) is the modulation scheme widely used in the fourth generation (4G) systems. In OFDM, the data is transmitted through closely spread out, narrow-band subcarriers. Using IFFT operation prevents interference between subcarriers. To maintain orthogonality between subcarriers, OFDM uses a Cyclic Prefix (CP). Besides, to reduce out-of-band emissions (OOB), windowing principle is used in OFDM prototype filter. All these advantages make from the OFDM the anchor waveform on to which other waveforms are derived. However, OFDM suffers from a lot of limitations that make it unsuitable for 5G applications (9) (10).

This work was supported by the Innov'COM Laboratory of Higher School of Telecommunication (Sup'Com), University of Carthage Tunisia.

Authors are with Sup'Com, University of Carthage, Tunisia (e-mail: mounira.laabidi@supcom.tn, ridha.bouallegue@supcom.tn).

Following are some of the drawbacks of OFDM modulation that make it not recommended for 5G applications. Firstly, OFDM signal suffers from high PAPR (Peak to Average Power Ratio) (9). Because of this, OFDM system requires a Power Amplifier (PA) with higher PAPR. Secondly, it is prone to ISI (Inter Symbol Interference) and ICI (Inter Carrier Interference) that require both time offset and frequency offset correction algorithms. Thirdly, since OFDM signal follows multiple paths and to avoid ISI errors due to timing offsets, the use of CP is compulsory. Consequently, that lead to loss of efficiency. All these limitations make OFDM non suitable for 5G upcoming applications.

To meet the requirements of the above-mentioned 5G upcoming applications, not long ago, several alternatives to OFDM technology which is incapable to meet the next generation telecommunication standards were suggested for the 5G air interface. These involve filtered OFDM (F-OFDM) (11), Filtered Bank Multi-Carrier (FBMC) (12), Generalized Frequency Division Multiplexing (GFDM) (13), and Universal Filtered Multi-Carrier (UFMC) (14) (15). In this paper, we focus on UFMC technology. The Universal Filtered Multi-Carrier (UFMC) (14) (15) is the new contender that is characterized by a better Out of Band (OOB) leakage suppression than CP-OFDM and higher spectral efficiency. It is a typical modulation based on sub-band filtering. It combats multi-user interference and presents a well short burst support (16). Moreover, it shows robustness against each of inter-carrier interference (ICI) and inter-symbol interference (ISI) as well it is suitable for low latency scenarios (17). Besides, UFMC can still use QAM, consequently, it supports diversity by an efficient Multiple Input Multiple Output (MIMO) integration.

Nonetheless, UFMC as a multi-carriers modulation, suffers from high Peak to Average Power Ratio (PAPR). Hence, it produces the saturation of the high-power amplifiers (HPA) and, consequently, introduces large performance degradation. To get along with this problem of linearity, two methods are possible: The first one which compensates the HPA non-linearity is called linearization and the second one is based on reducing the UFMC signal envelope fluctuation by using PAPR reduction methods. In this investigation we consider the PAPR reduction approach.

In the literature (18)-(19), few are the studies that consider the reduction of PAPR in UFMC systems. The PAPR reduction techniques that have been proposed for UFMC provide great results in reducing the PAPR. Most of these works deal with the probabilistic approaches such as Selective Mapping



(SLM) and Partial Transmit Sequence (PTS). In (18), authors proposed a PAPR reduction scheme based on Partial Transmit Sequence (PTS) for the UFMC waveform, which principle lie on the multiplication of phase factors by the subdivided data sub-blocks. Yet, because of the high number of inverse fast Fourier transform (IFFT) operations, this method reveals a higher computational complexity. Hence, in (20), a low complexity PTS method is advanced for UFMC signals.

In (21), a PAPR reduction scheme that combines non-linear and pre-coding companding techniques has been suggested and the ensuing PAPR reduction methods are compared in terms of both PAPR and BER performances. Besides, a new efficient piecewise nonlinear companding transform is proposed in (22), to reduce the PAPR in UFMC systems. The proposed companding method shows an effective trade-off between PAPR reduction and further system performance metrics like BER and OOB radiation. In (23),(24), Fathy *et al.* extend the SLM scheme initially suggested for OFDM to reduce the high PAPR of UFMC Signals, they propose a low-Complexity SLM PAPR Reduction approach for UFMC Systems, which is based on the linearity of the UFMC modulator. A novel PAPR reduction algorithm based on SLM technique in UFMC systems was also suggested in (19).

All the above-mentioned PAPR reduction schemes reduce the high PAPR of UFMC. The probabilistic approaches such as SLM and PTS introduce random phase shifts to the transmitted signal without producing signal distortion. However, these schemes reduce the spectral efficiency because of the side information (SI) which is communicated to the receiver to recover the original data.

To the best of our knowledge, no work deal with the adding signal-based approach like Tone reservation PAPR reduction scheme to reduce the envelope fluctuations of UFMC signals. Due to the huge number of benefits that distinguish the TR scheme, we concentrate on this technique to reduce the PAPR of the UFMC signal. The TR benefits consist in (i) an excellent performance in reducing PAPR without neither signal distortion nor BER degradation, (ii) the transparency to receiver as there is no need for side information transmission, and (iii) its ease and effectiveness.

In this investigation, we suggest two novel PAPR reduction schemes for UFMC signal. The anticipated schemes are TR based PAPR reduction schemes, initially proposed for OFDM. In the proposed algorithms, we use some tones of the zeros padding guard interval of each sub-band to carry the peak canceling signal that helps in reducing the envelope fluctuation of UFMC signal of sub-band b where b in $[1, \dots, B]$. The TR application with UFMC is tested before and after the filtering process.

The remainder of the paper is organized as follows. The second section describes both the UFMC and OFDM signals and some of their properties. The third section is devoted to describing the conventional TR scheme and sheds light on the proposed two PSTR PAPR reduction schemes for reducing the PAPR of the UFMC signal. The fourth section reports the simulation results regarding the performances of the proposed PAPR reduction schemes in terms of PAPR reduction ability, Bit Error Rate (BER) performance and Power Spectral Density

(PSD). This section includes the discussion of the obtained results. Finally, conclusions and perspectives are stated in the fifth section.

computational coprocessors in classical ICT systems, but so far only for a confined set of problems (?). Search goes on widening this set.

II. THEORY

A. UFMC and OFDM Systems Models

This section describes the block diagram of both UFMC transmitter and UFMC receiver and compares UFMC with OFDM where UFMC represents a generalization of FBMC and Filtered OFDM multi-carrier modulation schemes.

1) *UFMC Transmitter*: In UFMC transmitter side, at first, the information bits are mapped into M-ary quadrature amplitude modulation (M-QAM) symbols(e.g., $M = 4$). Therefore, N_{sc} symbols are grouped to form the entries of the whole vector to transmit where N_{sc} refers to the number of data subcarriers. Then, the whole bandwidth is divided into several sub-bands also called resource block (RB) where each sub-band contains some subcarriers. Then, instead of filtering each subcarrier individually like in the Filter bank multi-carrier (FBMC), filtering a group of subcarriers is done in this waveform. Hence, UFMC merges the advantages of OFDM in terms of orthogonality and filter bank in FBMC.

To suppress OOB leakage, UFMC use band-pass transmitter (Tx) filter where each RB has a matching Tx filter. Every band-pass Tx filter is designed to simply pass the designated RB. In UFMC system, to avoid Inter Symbol Interference (ISI) owing to Tx filter delay, a guard interval (GI) padded with zeros is introduced between the IFFT symbols. The block diagram of the UFMC transmitter is shown at Fig. 1.

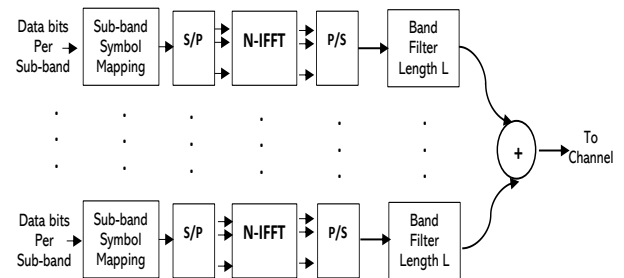


Fig. 1. UFMC Trasmmitter block diagram

At first, the whole band of subcarriers N_{sc} is partitioned into B sub-bands as shown in Fig. 2. Every sub-band has a fixed number of subcarriers ($N_b = N_{sc}/B$) and, for a given transmission, not all sub-bands should be employed. The new sub-sequence in sub-band b is defined as in equation (1):

$$X_b(k) = \begin{cases} 0 & 0 \leq k \leq w + (b-1) \frac{N_{sc}}{B} - 1 \\ X & w + (b-1) \frac{N_{sc}}{B} \leq k \leq w + b \frac{N_{sc}}{B} - 1 \\ 0 & (w+b) \frac{N_{sc}}{B} \leq k \leq (N-1) \end{cases} \quad (1)$$

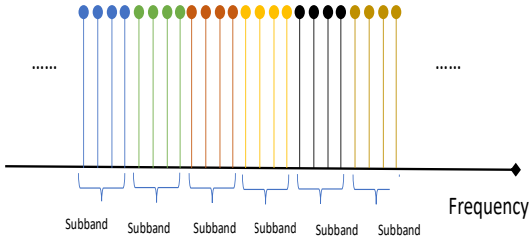


Fig. 2. Subband partition in UFMC system

Where $w = (N - N_{sc})/2$

Second, an N -point IFFT (exemplified by V matrix) for each sub-band is calculated, concerning the unallocated subcarriers zeros are inserted.

$$xx_b(k) = \frac{1}{\sqrt{N}} \sum_{k=0}^{N-1} X_b(k) \exp^{j \frac{2\pi k n}{N}} \quad (2)$$

with :

$$0 \leq n \leq N - 1; 1 \leq b \leq B \quad (3)$$

Where n and b respectively relate to the subcarrier and sub-band index. Third, each sub-band is filtered by a Dolph Chebyshev filter of length L (represented by a Toeplitz matrix F with dimensions $(N + L - 1) * N$).

$$x_b(k) = \sum_{l=0}^{L-1} xx_b(k-l) f_b(l) \quad (4)$$

with k in $[0, N + L - 1]$.

Finally, the different sub-bands responses are summed to form the multi-carrier signal to be transmitted. The UFMC transmitted signal of duration $(N + L - 1)$ can be given as in equation (5):

$$x(k) = \sum_{b=1}^B F_{b,k} V_{b,k} X_{b,k} \quad (5)$$

For sub-band b where b in $1, \dots, B$, $F_{b,k}$ is the filter impulse response, performing the linear convolution, see equation (5), $V_{b,k}$ represents the IFFT matrix and $X_{b,k}$ denotes the data blocks.

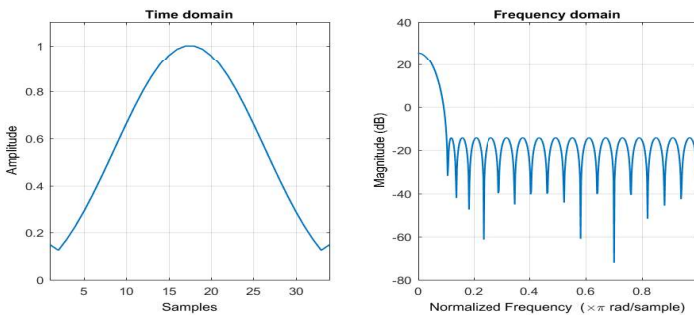


Fig. 3. Impulse Response of the Dolph-Chebyshev Filter

In this paper, the optimal Dolph Chebyshev filter was considered for sub-band filtering (25),(26). The filter length is L

which depends upon the sub-band size. The Dolph-Chebyshev window is constructed in the frequency domain by taking samples of the window's Fourier transform. Dolph Chebyshev window is used in spectral analysis and FIR filtering. It has special features, for a given ripple ratio and filter length L it has narrow main lobe width and it contains equi-ripple side lobe level (SLL). Fig. 3 highlights the filter impulse response.

2) *UFMC Receiver*: The received signal from the channel follows several operations. Firstly, the received vector is padded to twice the FFT length then FFT is calculated followed by downsampling process. Secondly, a per-subcarrier equalization is performed for equalizing the combined outcome of the channel and the sub-band filtering. Besides, the receiver utilizes just the even subcarriers to recover the signal and avoids the odd one of the $2 \times$ size FFT. After a parallel to serial conversion, a symbol demapping operation is required to recover the transmitted data bits.

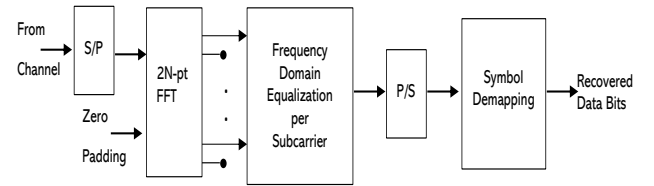


Fig. 4. UFMC Receiver Block Diagram

3) *OFDM transceiver*: The OFDM transceiver is composed of the transmitting and the receiving sides. Fig. 5 presents the main components of the OFDM system. As shown in Fig. 5, the modulator and demodulator are respectively implemented by the Inverse Fast Fourier Transform (IFFT) and the Fast Fourier Transform (FFT) blocks. To maintain orthogonality between subcarriers, OFDM adds a CP at the transmitter side and removes it at the receiver one.

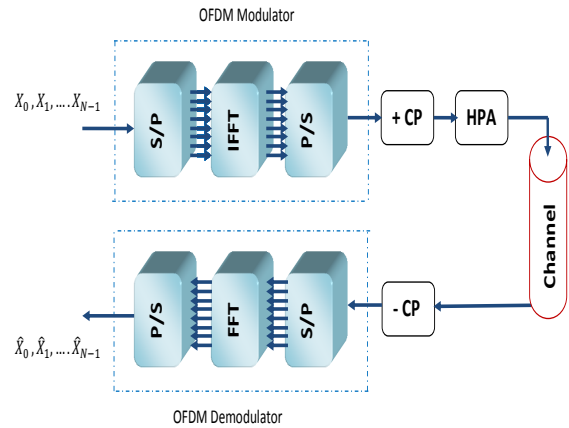


Fig. 5. OFDM Transmission Chain.

In the OFDM case, the sub-channels are characterized by orthogonality. An OFDM signal is the sum of N independent Quadrature Amplitude Modulation(QAM) symbols mapped onto N different sub-channels with $\frac{m}{T}$ frequency separation where T is the OFDM symbol period. Thus, $f_m = f_c + \frac{m}{T}$

where f_c is the carrier frequency. If we consider $x_{m,n}$ as the OFDM symbol to transmit at instant nT on the m th subcarrier, the transmitted baseband signal can be written as in (27):

$$s(t) = \frac{1}{\sqrt{N}} \sum_{m=0}^{N-1} \sum_{n=-\infty}^{\infty} x_{m,n} f(t - nT) e^{j \frac{2\pi}{T} mt} \quad (6)$$

where N is the number of subcarriers, T is the OFDM symbol period, $x_{m,n}$ is a complex-valued symbol transmitted on the m th subcarrier and at the instant nT , and in this first equation, the factor $\frac{1}{\sqrt{N}}$ is introduced for power normalization and $f(t)$ is the pulse shape of the OFDM scheme which is a rectangular window function defined as in (7):

$$f(t) = \begin{cases} 1, & 0 \leq t < T \\ 0, & \text{Otherwise} \end{cases} \quad (7)$$

The OFDM modulated signal $s(t)$ is the sum of independent identically distributed random variables. According to the central limit theorem, if the number of subcarriers is large enough, the signal can be approximated as a complex Gaussian distributed random variable.

B. Tone Reservation-Based PAPR reduction scheme in UPMC Signal

1) *Reminder of Conventional Tone Reservation*: The Tone Reservation TR PAPR reduction scheme was firstly introduced by Tellado and Cioffi in(28)(29). Such design can be in fact classified as an adding and clipping-based PAPR reduction scheme.

The conventional TR-clipping based PAPR reduction technique applies a hard clipping to the input OFDM signal. Then, the correction signal or peaks reduction signal is deduced by subtracting the clipped signal from the input signal. After that, and to comply with the TR concept the correctional signal is passed to an FFT/IFFT block

The main idea of this scheme is to reduce the envelope fluctuations of the MCM signal s_n by adding a peaks reduction signal c_n . Working with an OFDM system using N subcarriers, the principle of TR is to reserve N_{PRTs} sub-carriers among N to carry the PAPR reduction or the correctional signal. The $N_{data} = N - N_{PRTs}$ sub-carriers are used for transmitting the data signal. The output of the TR PAPR reduction block can be expressed as $s_n + c_n$ where c_n is the peaks reduction and the time domain signal of C and s_n is the time domain signal of S .

In TR, S and C are constrained to lie in disjoint frequency subspaces so that their additional signals cause no distortion on the data-bearing subcarriers. More precisely, if we consider N_{data} as the size of data-bearing subcarriers and N_{PRTs} as the size of reserved PRTs (non-data-bearing subcarriers). It is then reasonable that with TR, or generally for any adding signal PAPR reduction scheme, the PAPR is redefined as in equation (8):

$$PAPR_{[s]} = \frac{\max_{n \in [0, N-1]} |s(n) + c(n)|^2}{E[|s(n)|^2]} \quad (8)$$

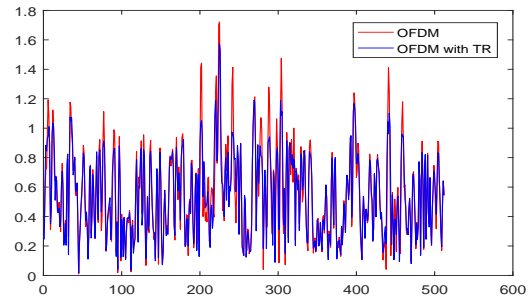


Fig. 6. OFDM signals with and without TR

As equation (8) shows, the choice of the additive signal c_n affects the PAPR of the whole information-carrying. Since PRTs are only used for reducing PAPR. Therefore, no side information is required in the receiver side, only the receiver must ignore the contents of the reserved PRTs. Consequently, no BER degradation will be considered. Fig. 6 represents both the OFDM signals: in red color OFDM without correction and in blue color OFDM with reduced peaks. It is clear from Fig. 6 that when adding a correctional signal to the OFDM one, the amplitude of this latter will be reduced and therefore the high peaks.

To evaluate the performance of any PAPR reduction method, the Complementary Cumulative Distribution Function (CCDF) is one of the most useful informative metrics. CCDF is the probability that PAPR exceeds a given PAPR threshold.

2) *Per Sub-band Tone Reservation (PSTR) for UPMC*: In UPMC, the data symbols are firstly divided and individually introduced to N point IFFT blocks, called resource blocks (RB) then each RB is filtered individually. Finally, all RB are consolidated to form an UPMC symbol. So we propose a method that applies the TR scheme to each resource block to form a low PAPR combination of B RB. The originality of the suggested Per Sub-band Tone Reservation (PSTR) for UPMC consists in randomly choosing the PRTs position for each RB in the out-of-band zone or in the zeros padding guard interval of each sub-band. If we denote N_b as the sub-band size, then there are $N - N_b$ positions from which we can randomly select the PRTs. As depicted in Fig. 7 The PRTs are randomly selected in both the green circles.

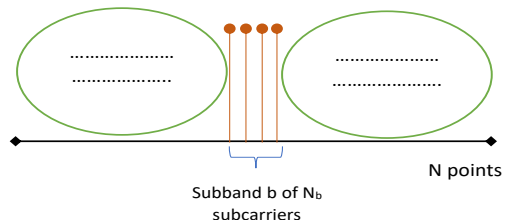


Fig. 7. The principle of PSTR PRTs selection

PrePSTR scheme for UPMC The first proposed PAPR reduction scheme is called pre-filtering PSTR (PrePSTR) algo-

rithm. It uses the least squares approximation (LSA) algorithm to calculate the optimization factor (μ) that multiplies the peak-canceling signal, to reduce the PAPR of the UPMC signal. Fig. 8 shows the position of the aforementioned PSTR PAPR reduction scheme in the transmission chain of one sub-band.

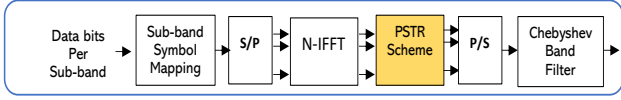


Fig. 8. Pre-filtering PSTR block diagram

The prePSTR suggested scheme consists in the following operations;

For sub-band b where b in $1, \dots, B$.

- 1) Start with the time domain signal in sub-band (b) $xx_b(k)$ as introduced in equation (2) ;
- 2) Associate a value to iteration number $iternum$
- 3) Based on a predefined threshold A , clip $xx_b(k)$ to get the thresholded signal y of the RB number b as shown by equation (9):

$$y_k = \begin{cases} xx_b(k), & |xx_b(k)| \leq A \\ Ae^{j\Theta_k}, & |xx_b(k)| > A \end{cases} \quad (9)$$

- 4) Compute the clipped portion of the signal as follows:

$$c_{clip} = y_k - xx_b(k) \quad (10)$$

- 5) Demodulate the clipping noise signal to get C_{clip} .
- 6) In the PRTs positions, keep the components of C_{clip} which figure in and fix the rest to zeros;
- 7) Modulate the frequency domain signal C_{clip} by performing IFFT operator to get c the peaks reduction signal;
- 8) Compute the new time domain signal of sub-band b after IFFT process as follows:

$$xx_b(k)^{i+1} = xx_b(k)^i + \mu * c_k \quad (11)$$

where: k in $[0, N + L - 1]$ and μ is the step of the LSA method.

The algorithm should be running until no point to clip or the number of TR iterations expires. Then the output signal is introduced to the adequate band-pass Chebyshev filter to have the UPMC signal of sub-band (b). PostPSTR scheme for UPMC The second proposed PAPR reduction scheme called post-filtering PSTR (PostPSTR) algorithm calculates the peaks reduction signal of sub-band b from the UPMC time domain signal as in equation (4). It is called PostPSTR because the PSTR block is inserted after the process of filtering. All the aforementioned steps of PrePSTR are applied with the PostPSTR scheme. The clipped signal is calculated from the resulting signal of the Chebychev band filter. Fig. 9 shows the position of the PostPSTR PAPR reduction scheme in the transmission chain of one sub-band.

III. EXPERIMENT

In this section we examine the performance of both UPMC and OFDM systems. To evaluate the performances of UPMC

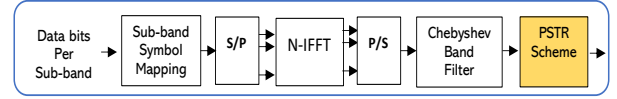


Fig. 9. Post-filtering PSTR block diagram

we developed a simulation model using MATAB. Simulation parameters are shown in Table I. The PAPR reduction capabilities of the above-mentioned two PSTR method (i.e. PrePSTR and PostPSTR) being suggested for UPMC are verified through simulations. Accordingly, the complementary cumulative distribution function (CCDF) diagrams of the PSTR techniques, the Bit Error Rate (BER), and the Power Spectral Density (PSD) ones all being used to compare both UPMC and OFDM systems are depicted. Concerning the PRTs, the positions are randomly selected since contiguous and equally spaced positions have no impact on PAPR gain.

TABLE I
SIMULATION PARAMETERS

Parameter	Value
FFT size, N	512
Modulation order, M	2
Number of subbands, B	10
Subband size, N_b	20
Modulation scheme	QAM
Filter	Dolph-chebychev
Filter Length, L	43
Side-lobe attenuation	40 dB
Number of data subcarriers N_{sc}	200
PRTs number for OFDM	80
PRTs number per subband	8

A. Power Spectral Density comparisons

Power Spectral Density displays the strength of the energy variation as a function. Power spectral density of the UPMC transmit signal is designed to give low out-of-band leakage. Fig. 10 shows the spectral densities of UPMC and OFDM schemes for 200 subcarriers.

In UPMC, the overall band is divided into 10 sub bands, each sub band having 20 subcarriers with less side lobes. Because of filtered operation for each sub-band in UPMC, we can observe that the spectral re-growth is (-80 dB) which is very low as compared to that of OFDM (-40 dB). Hence, the UPMC scheme is more advantageous when compared to OFDM as it provides higher spectral efficiency. UPMC has lower side lobes, so it allows better utilization of the allocated spectrum. Thus, it is safe to conclude that UPMC ranks better than CP-OFDM in terms of PSD.

B. CCDFs comparisons

In this sub-section we evaluate the performance of both PrePSTR and PostPSTR PAPR reduction schemes being suggested for UPMC in terms of CCDFs.

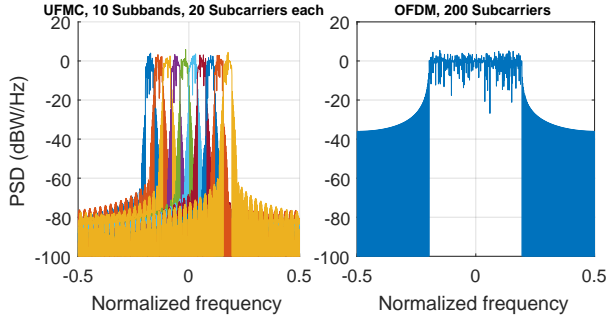


Fig. 10. Power Spectral Density comparisons between UFMC and OFDM

The CCDFs plot of the UFMC and OFDM systems, with and without PAPR reduction, are illustrated in Fig.11. The numerical values for PAPR are shown in Table I. The Reserved tones R are randomly set for each sub-band. With reference to Fig.11 and Table I, we can recognize that the proposed PrePSTR PAPR reduction methods considerably reduce the PAPR of the UFMC signal with only one iteration. We have also simulated the PrePSTR scheme with contiguous positions of PRTs and with equally spaced PRTs but the results prove no improvement in term of PAPR.

TABLE II
SIMULATION RESULTS

	Gradient-TR for OFDM	PrePSTR for UFMC
Iterations number	1	1
PAPR/CCDF of 10^{-3}	8 [dB]	5.2 [dB]
	Clipping-TR for OFDM	PSTR for UFMC
Iterations number	30	1
PAPR/CCDF of 10^{-3}	6 [dB]	5.2 [dB]

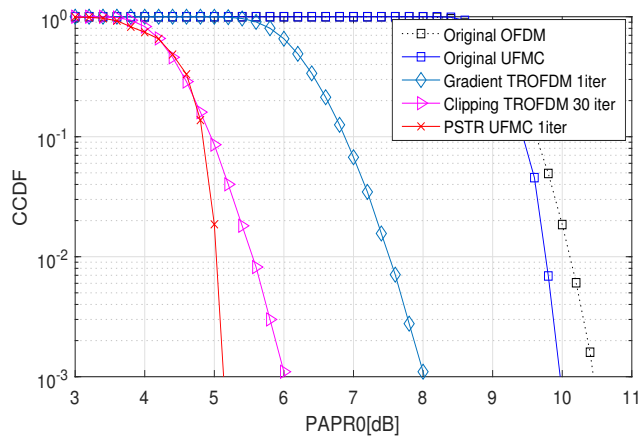


Fig. 11. CCDF comparisons between UFMC and OFDM when using TR algorithm

As mentioned in Table II, at the level of 10^{-3} , the PrePSTR PAPR reduction scheme suggested for UFMC with just one iteration outperforms the conventional clipping-based TR with 30 iteration of about 1 dB and outperforms the gradient-based method with one iteration of about 3 dB. Therefore, with the LSA-based PrePSTR scheme, we could obtain a significant PAPR reduction with low complexity. In other words, with just one iteration, the amplitudes of the peak-canceling signal generated by the LSA-based PrePSTR technique, are practically equivalent to those of the original clipping noise.

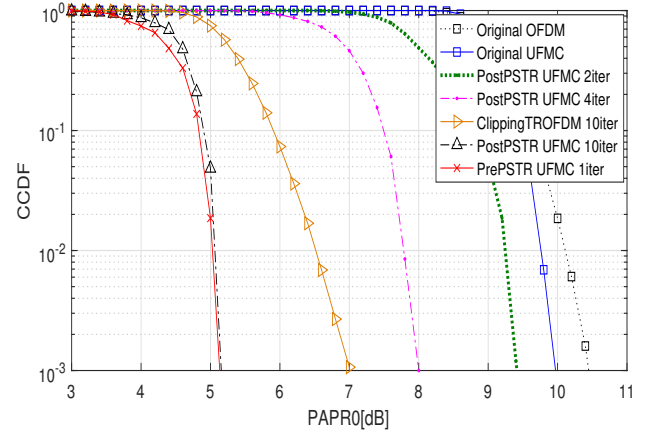


Fig. 12. CCDF comparisons when using Clipping TR for OFDM and PostPSTR for UFMC

In Fig.12, the performance of PostPSTR technique on reducing the PAPR of original UFMC signal is investigated. As can be clearly seen from the Fig.12, the PAPR reduction performance of the PostPSTR technique improves significantly with the increase in the TR iterations number.

C. BER comparisons

Fig. 13 compares the BER performance of the UFMC signal without and with the PSTR scheme, where the PRTs are randomly selected and reserved for the PAR reduction over an AWGN channel. Table III presents the BER values with respect to the SNR in [dB] of both UFMC signals with and without PSTR PAPR reduction scheme. As it is clear from Fig. 13 and Table III in an AWGN channel, the PSTR has no strong effect on the BER performance of the UFMC system.

TABLE III
BER PERFORMANCE OF PSTR SCHEME WITH QPSK MODULATION OVER AWGN CHANNEL

SNR values [dB]	UFMC BER	BER of UFMC with PSTR
1	0.045	0.08
2	0.0275	0.0475
3	0.0275	0.0475
4	0.02	0.0375
5	0.005	0.02
6	0.005	0.0125
7	0.0025	0.0075
> 7	0	0

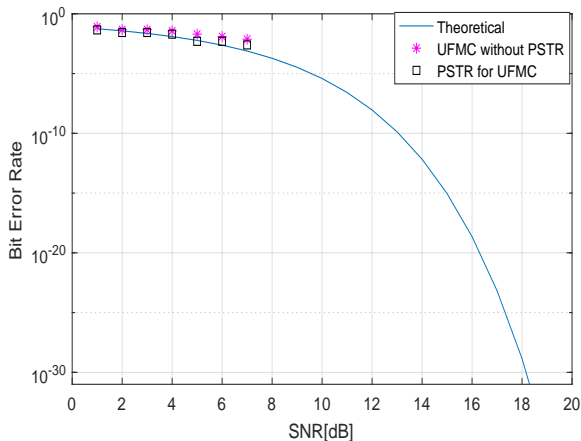


Fig. 13. BER performance of the PSTR scheme over AWGN channel

IV. CONCLUSIONS

In this paper, to solve the issue of high PAPR of UFMC signal, two PAPR reduction techniques, called Pre and Post PSTR were proposed. The proposed PSTR methods are TR-based. Since TR requires several subcarriers called PRTs to carry the correctional signal and, to not use the data bearing subcarriers as PRTs, our suggested schemes install PRTs in the side of guard interval tones. The analysis proved that the PSTR techniques improve PAPR reduction compared to a normal UFMC system. Moreover, a detailed comparison of the BER of the proposed PSTR PAPR reduction method is also presented. The analysis prove that the suggested PSTR method preserves the BER performance of the standard UFMC system on the AWGN channel. The PSTR achieves about 5 dB over the conventional TR for OFDM to decrease the PAPR of the transmitted UFMC waveform for only one TR iteration. Simulation results confirm the huge number of benefits that distinguish the TR scheme, and show a large performance improvement over other state-of-the-art methods being suggested for UFMC in terms of both PAPR reduction and BER measurements .

REFERENCES

- [1] J. Navarro-Ortiz, P. Romero-Diaz, S. Sendra, P. Ameigeiras, J. J. Ramos-Munoz, and J. M. Lopez-Soler, "A survey on 5g usage scenarios and traffic models," *IEEE Communications Surveys Tutorials*, vol. 22, no. 2, pp. 905–929, 2020. [Online]. Available: <https://doi.org/10.1109/COMST.2020.2971781>
- [2] S. Chen, J. Hu, Y. Shi, Y. Peng, J. Fang, R. Zhao, and L. Zhao, "Vehicle-to-everything (v2x) services supported by lte-based systems and 5g," *IEEE Communications Standards Magazine*, vol. 1, no. 2, pp. 70–76, 2017. [Online]. Available: <https://doi.org/10.1109/MCOMSTD.2017.1700015>
- [3] G. Premsankar, M. Francesco, and T. Taleb, "Edge computing for the internet of things: A case study," *IEEE Internet of Things Journal*, vol. PP, pp. 1–1, 02 2018. [Online]. Available: <https://doi.org/10.1109/JIOT.2018.2805263>
- [4] M. Series, "Imt vision—framework and overall objectives of the future development of imt for 2020 and beyond," R. ITU, Ed., 2015.
- [5] Z. E. Ankarali, B. Peköz, and H. Arslan, "Flexible radio access beyond 5g: A future projection on waveform, numerology, and frame design principles," *IEEE Access*, vol. 5, pp. 18 295–18 309, 2017. [Online]. Available: <https://doi.org/10.1109/ACCESS.2017.2684783>
- [6] Y. Medjahdi, S. Traverso, R. Gerzaguët, H. Shaïek, R. Zayani, D. Demmer, R. Zakaria, J.-B. Doré, M. Ben Mabrouk, D. Le Ruyet, Y. Louët, and D. Roviras, "On the road to 5g: Comparative study of physical layer in mtc context," *IEEE Access*, vol. 5, pp. 26 556–26 581, 2017. [Online]. Available: <https://doi.org/10.1109/ACCESS.2017.2774002>
- [7] B. Farhang-Boroujeny and H. Moradi, "Ofdm inspired waveforms for 5g," *IEEE Communications Surveys Tutorials*, vol. 18, no. 4, pp. 2474–2492, 2016. [Online]. Available: <https://doi.org/10.1109/COMST.2016.2565566>
- [8] X. Cheng, Y. He, B. Ge, and C. He, "A filtered ofdm using fir filter based on window function method," in *2016 IEEE 83rd Vehicular Technology Conference (VTC Spring)*, 2016, pp. 1–5. [Online]. Available: <https://doi.org/10.1109/VTCSpring.2016.7504065>
- [9] F. Schaich and T. Wild, "Waveform contenders for 5g—ofdm vs. fbmc vs. ufmc," in *2014 6th International Symposium on Communications, Control and Signal Processing (ISCCSP)*, 2014, pp. 457–460. [Online]. Available: <https://doi.org/10.1109/ISCCSP.2014.6877912>
- [10] C. Nie and Y. Bai, "Papr reduction with amplitude clipping and subband filter in filtered-ofdm system," booktitle="5g for future wireless networks," K. Long, V. C. Leung, H. Zhang, Z. Feng, Y. Li, and Z. Zhang, Eds. Cham: Springer International Publishing, 2018, pp. 220–227.
- [11] L. Zhang, A. Ijaz, P. Xiao, M. M. Molu, and R. Tafazolli, "Filtered ofdm systems, algorithms, and performance analysis for 5g and beyond," *IEEE Transactions on Communications*, vol. 66, no. 3, pp. 1205–1218, 2018. [Online]. Available: <https://doi.org/10.1109/TCOMM.2017.2771242>
- [12] A. Bedoui and M. Et-tolba, "A comparative analysis of filter bank multicarrier (fbmc) as 5g multiplexing technique," in *2017 International Conference on Wireless Networks and Mobile Communications (WINCOM)*, 2017, pp. 1–7. [Online]. Available: <https://doi.org/10.1109/WINCOM.2017.8238200>
- [13] G. Fettweis, M. Krondorf, and S. Bittner, "Gfdm - generalized frequency division multiplexing," in *VTC Spring 2009 - IEEE 69th Vehicular Technology Conference*, 2009, pp. 1–4. [Online]. Available: <https://doi.org/10.1109/VETECS.2009.5073571>
- [14] V. Vakilian, T. Wild, F. Schaich, S. ten Brink, and J.-F. Frigon, "Universal-filtered multi-carrier technique for wireless systems beyond lte," in *2013 IEEE Globecom Workshops (GC Wkshps)*, 2013, pp. 223–228.

- [Online]. Available: <https://doi.org/10.1109/GLOCOMW.2013.6824990>
- [15] M. Mukherjee, L. Shu, V. Kumar, P. Kumar, and R. Matam, "Reduced out-of-band radiation-based filter optimization for ufmcs systems in 5g," in *2015 International Wireless Communications and Mobile Computing Conference (IWCMC)*, 2015, pp. 1150–1155. [Online]. Available: <https://doi.org/10.1109/IWCMC.2015.7289245>
- [16] I. Baig, U. Farooq, N. U. Hasan, M. Zghaibeh, A. Sajid, and U. M. Rana, "A low papr dht precoding based ufmcs scheme for 5g communication systems," in *2019 6th International Conference on Control, Decision and Information Technologies (CoDIT)*, 2019, pp. 425–428. [Online]. Available: <https://doi.org/10.1109/CoDIT.2019.8820502>
- [17] R. S. Yarrabothu and U. R. Nelakuditi, "Optimization of out-of-band emission using kaiser-bessel filter for ufmcs in 5g cellular communications," *China Communications*, vol. 16, no. 8, pp. 15–23, 2019. [Online]. Available: <https://doi.org/10.23919/JCC.2019.08.002>
- [18] N. Taşpinar and Şimşir, "Papr reduction based on partial transmit sequence technique in ufmcs waveform," in *2019 14th Iberian Conference on Information Systems and Technologies (CISTI)*, 2019, pp. 1–6. [Online]. Available: <https://doi.org/10.23919/CISTI.2019.8760726>
- [19] Y. Zhang, K. Liu, and Y. Liu, "A novel papr reduction algorithm based on slm technique in ufmcs systems," in *2018 IEEE/CIC International Conference on Communications in China (ICCC Workshops)*, 2018, pp. 178–183. [Online]. Available: <https://doi.org/10.1109/ICCCChinaW.2018.8674491>
- [20] W. Rong, J. Cai, and X. Yu, "Low-complexity pts papr reduction scheme for ufmcs systems," *Cluster Computing*, vol. 20, no. 4, pp. 3427–3440, 2017.
- [21] A. F. Imutairi, M. Al-Gharabally, and A. Krishna, "Performance analysis of hybrid peak to average power ratio reduction techniques in 5g ufmcs systems," *IEEE Access*, vol. 7, pp. 80 651–80 660, 2019. [Online]. Available: <https://doi.org/10.1109/ACCESS.2019.2916937>
- [22] K. Liu, Y. Ge, and Y. Liu, "An efficient piecewise nonlinear companding transform for papr reduction in ufmcs systems," in *2019 IEEE/CIC International Conference on Communications in China (ICCC)*, 2019, pp. 730–734. [Online]. Available: <https://doi.org/10.1109/ICCCChina.2019.8855924>
- [23] S. A. Fathy, M. N. A. Ibrahim, S. S. Elagooz, and H. M. El-Hennawy, "Efficient slm technique for papr reduction in ufmcs systems," in *2019 36th National Radio Science Conference (NRSC)*, 2019, pp. 118–125. [Online]. Available: <https://doi.org/10.1109/NRSC.2019.8734569>
- [24] S. A. Fathy, M. Ibrahim, S. El-Agooz, and H. El-Hennawy, "Low-complexity slm papr reduction approach for ufmcs systems," *IEEE Access*, vol. 8, pp. 68 021–68 029, 2020. [Online]. Available: <https://doi.org/10.1109/ACCESS.2020.2982646>
- [25] R. Nissel, S. Schwarz, and M. Rupp, "Filter bank multicarrier modulation schemes for future mobile communications," *IEEE Journal on Selected Areas in Communications*, vol. 35, no. 8, pp. 1768–1782, 2017. [Online]. Available: <https://doi.org/10.1109/JSAC.2017.2710022>
- [26] F. Harris, "On the use of windows for harmonic analysis with the discrete fourier transform," *Proceedings of the IEEE*, vol. 66, no. 1, pp. 51–83, 1978. [Online]. Available: <https://doi.org/10.1109/PROC.1978.10837>
- [27] H. S. Hussein, A. S. Mubarak, O. A. Omer, U. S. Mohamed, and M. Salah, "Sparse index ofdm modulation for iot communications," *IEEE Access*, vol. 8, pp. 170 044–170 056, 2020. [Online]. Available: <https://doi.org/10.1109/ACCESS.2020.3024157>
- [28] J. Tellado and J. Cioffi, "Efficient algorithms for reducing par in multicarrier systems," in *Proceedings. 1998 IEEE International Symposium on Information Theory (Cat. No.98CH36252)*, 1998, pp. 191–. [Online]. Available: <https://doi.org/10.1109/ISIT.1998.708789>
- [29] —, "Peak-to-average power ratio reduction for multicarrier communication systems," 1999.